Randomly Constrained Orientational Order in Porous Glass

G. S. Iannacchione,[1,2] G. P. Crawford,[2] S. Žumer,[2,*] J. W. Doane,[1,2] and D. Finotello[1,2]

[1]*Department of Physics, Kent State University, Kent, Ohio 44242*
[2]*Liquid Crystal Institute, Kent State University, Kent, Ohio 44242*

(Received 10 June 1993)

Magnetic resonance and calorimetric studies of 4′-*n*-pentyl-4-cyanobiphenyl confined to Vycor glass, a random network of pores with average diameter ~70 Å, are reported. Under such severely constrained conditions, the nematic-to-isotropic transition is replaced by a continuous evolution of orientational order in the pores. Our findings are explained by a Landau type of model where the liquid crystal is confined to independent pore segments, suggesting that the glassylike orientational order is to a large extent locally determined.

PACS numbers: 61.30.Gd, 64.70.Md, 76.60.−k

The study of finite size effects on the behavior at phase transition for fluids confined to randomly connected pore networks has been an area of fruitful research. Interesting phenomena have been unveiled by probing the effects on the critical behavior of ^{4}He at the superfluid transition in porous glasses [1]. Equally appealing results were obtained through studies of the phase separation of binary liquid mixtures confined to porous glasses [2].

An emerging and rich area of research includes orientational order and phase transition studies of liquid crystals constrained by symmetry breaking confinements. The reasons are that the surface effect on the orientational molecular order is of long range in contrast to normal liquids, that they exhibit a variety of phase transitions which are experimentally accessible, and their potential for applications. The prediction of Sheng [3] for a nematic confined between two parallel ordering walls that the weakly first order nematic-isotropic (NI) transition is replaced by a continuous evolution of nematic order at a critical enclosure size was extended to spherically confined systems [4]. Experimentally, deuterium nuclear magnetic resonance (^{2}H-NMR) on spherical liquid crystal droplets as small as 200 Å in diameter proved the validity of Sheng's prediction [5]. In cylindrical geometries, ^{2}H-NMR was used to study director fields, measure surface parameters [6], and probe surface-induced order above the bulk transition [7]. Calorimetric studies found deviations from bulk behavior strongly dependent on surface anchoring and on the order of the transition [8].

Recently, studies have been extended to randomly confined systems. Light scattering and calorimetry for octylcyanobiphenyl (8CB) in silica Aerogel [a glass with a three dimensionally (3D) connected network of pores] showed that nematic ordering does not occur via a first order phase transition: Ordering is continuous with the correlation length not exceeding the pore size; the second order smectic-*A*-nematic (*A*N) transition was absent or greatly broadened [9]. Quasielastic light scattering measurements [10] suggest that the effect of the porous network on the nematic phase can be explained by a model developed for magnets with "random uniaxial anisotropies" predicting a first order transition from a disordered to a glassy state [11]. These studies stimulated theoretical work [12], showing that such systems are analogous to a magnetic spin system with "random fields" [13] rather than to one with "random anisotropies." Similar confinement effects as induced by a (solubilized) polymer on the lyotropic and thermotropic nematic phases have also been studied [14].

To understand the effects of confinement on the nematic phase, we studied pentylcyanobiphenyl (5CB) in the random network of pores in Vycor glass, using ^{2}H-NMR and calorimetry. From a transmission electron microscope photograph [15], Vycor can be described as a network of 3D randomly connected pore segments (inset to Fig. 1) with relatively uniform diameter $d \sim 70$ Å and average length $l \sim 300$ Å. The nematic correlation length [16] at the weakly first order NI transition is finite (~200 Å) and larger than the pore diameter. The severe confinement yields an inhomogeneous and depressed nematic orientational order which is intermediate between the nematic and the isotropic phases. No evidence for the NI transition was found. Using a Landau type of model, we present the first quantitative description of the effects of the confining geometry on the liquid crystal behavior.

For a typical Vycor sample, after thorough cleaning in an ultrasonic 30% hydrogen peroxide bath and pumping while heating, it was left overnight in isotropic 5CB, to ensure complete filling.

Orientational order is directly probed with ^{2}H-NMR. The quadrupole splitting frequencies of a ^{2}H on a 5CB-ad_2 molecule (deuterated on the first position of the hydrocarbon chain) located at $\mathbf{r}$ can be written as

$$\Delta\nu = (\mathbf{iQi})\Delta\nu_0 , \qquad (1)$$

where the tensor order parameter $\mathbf{Q}(\mathbf{r})$ describes the time average of the local orientational order [16], the unit vector $\mathbf{i}$ indicates the direction of the applied magnetic field, and $2\Delta\nu_0 \sim 175$ kHz, the ^{2}H quadrupole coupling constant. The observed spectral distribution (sum of all ^{2}H contributions) is expected to be partially time averaged due to the translational diffusion of the molecules [7].

^{2}H-NMR line shapes for 5CB-ad_2 in Vycor, at several temperatures bracketing the bulk NI transition ($T_{\rm NI} = 308$ K), are shown in Fig. 1. The quadrupolar splitting

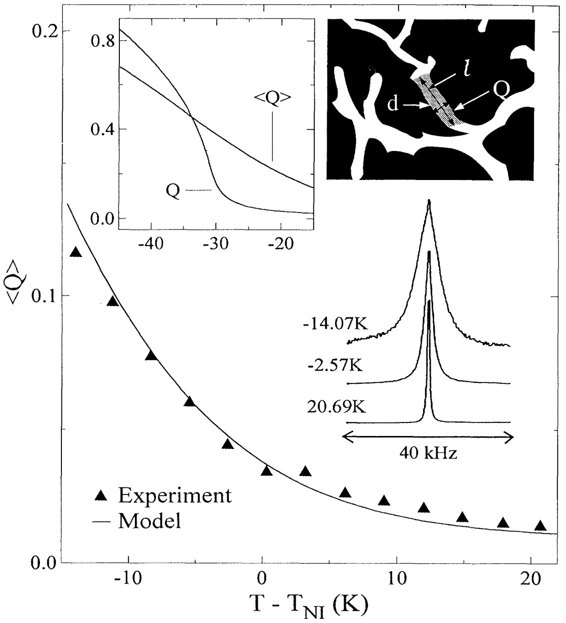

FIG. 1. Average order parameter as a function of temperature. Solid line through the linewidth data ($2\langle\Delta\nu\rangle/\Delta\nu_0$) is the model prediction. Also shown are ^{2}H-NMR line shapes for 5CB in Vycor at $T-T_{\rm NI}$ equal to -14.07, -2.57, and 20.69 K. Only a single absorption peak, and no quadrupole splitting typical of a nematic, is found. Left inset: Wider range model prediction for the temperature dependence of Q for $h/2a=h_0/2a=33$ K and $\langle Q\rangle$ for the same parameters and width distribution $2\sigma/a=17$ K. Right inset: Schematic representation of the Vycor structure. d and l are the diameter and length, while Q is the effective order parameter in a particular pore segment.

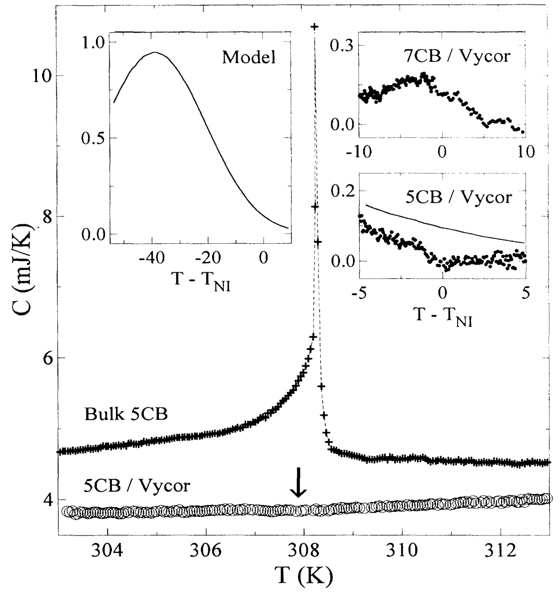

FIG. 2. Heat capacity against temperature for 5CB in Vycor (○) and for a 2.4 mg (scaled from a run that used 4 mg) bulk sample (+). Indicated by the arrow, only a subtle break at 307 K and no heat capacity peak is seen. For clarity, a dashed line is drawn through the bulk data. Left inset: Prediction from our model for the specific heat behavior. Right insets: Results for 5CB (solid line is the model prediction using parameters from the NMR fit) and 7CB, after subtracting the high temperature dependence to emphasize the low temperature rise (5CB) and the bump (7CB) in the specific heat as predicted by our model. $T_{\rm NI}$ is the bulk transition temperature. For all insets, the vertical axis is ΔC in mJ/K and the horizontal axis is temperature in K.

typical of the nematic phase is not found. At $T-T_{\rm NI}=-14.07$ K, a single central absorption peak of linewidth $\langle\Delta\nu\rangle\sim5.8$ kHz (FWHM) is measured. As the temperature is increased the linewidth $\langle\Delta\nu\rangle$ continuously decreases to 0.7 kHz for $T-T_{\rm NI}=20.69$ K. Although a single central absorption peak is typical of an isotropic fluid, $\langle\Delta\nu\rangle$ for 5CB in Vycor is nearly 20 times larger (20.69 K above $T_{\rm NI}$) than the measured isotropic bulk 5CB-αd_2 linewidth. Since the magnetic coherence length (~1.2 μm) [16] is much larger than the pore size, the magnetic field has a negligible effect on the nematic order in the pores. The spectral patterns, independent of the direction of the applied field, confirmed the random nature of the porous Vycor network.

A single broad absorption peak may be attributed to diffusion-induced motional averaging over randomly oriented nematic domains, to a distribution of weakly ordered nematic areas, or more realistically, to some intermediate case. To see which situation applies, we note that the modulation of the quadrupolar coupling induced by translational self-diffusion of liquid crystal molecules among pore segments of length l is characterized by a time $\tau_0\sim l^2/2D$, with D the effective diffusion constant. The diffusion is certainly hindered by surface interactions causing possible bonding of the molecules to the glass surface as observed in other systems [7,17].

Using a typical bulk value of 10^{-11} m^2/s for D [7,17] we obtain an overestimate for the diffusion-induced modulation rate: $\tau_0^{-1}\sim2\times10^4$ s^{-1}. A modulation at such a rate can affect the spectra when $\Delta\nu<1/2\pi\tau_0$ [18]. Here, only far above $T_{\rm NI}$, where $\langle\Delta\nu\rangle<1$ kHz, is this condition realized. For the fluctuating quadrupolar coupling with amplitude ω_q, one can use $T_2^{-1}\sim\omega_q^2\tau_0$ to estimate the width of the resonance line [18]. In Vycor, for $\omega_q=\pi\langle\Delta\nu\rangle$, a broadening much smaller than $\langle\Delta\nu\rangle$ is found at all temperatures. Thus, to a good approximation, the ^{2}H-NMR spectrum reflects the distribution of the independent contributions from pore segments. Each contribution is motionally averaged over the suppressed nematic order in the corresponding pore segment.

The lack of evidence for the NI transition in the ^{2}H-NMR spectra suggests that no heat capacity peak should be found. This was confirmed using ac calorimetry [8,19] to measure the heat capacity for 5CB in Vycor, shown in Fig. 2. The Vycor piece (10.6 mg), whose contribution has been subtracted, contained about 2.5 mg of 5CB. Within our resolution, no signature was seen over the temperature range probed. A linear heat capacity, changing slope just below the bulk $T_{\rm NI}$ (arrow in Fig. 2), was found. For comparison, results for a bulk 5CB sample are included in Fig. 2. As shown in the inset to Fig. 2, when the heat capacity studies were repeated for heptylcyanobiphenyl (7CB) in Vycor (wider nematic range and higher $T_{\rm NI}$), a greatly suppressed and broadened heat capacity bump, over 20 K wide, was seen.

To establish how much of the orientational order is influenced by the local size and shape of a pore segment, and how much by the interaction between the liquid crystal in different segments of the network, we estimate the ratio of the surface of a glass-liquid-crystal interface in a pore segment (l) to the surface at the ends of the segment where the liquid crystal is connected to an adjacent segment (d). See inset to Fig. 1. The ratio $l/d \sim 4$ suggests that our system can be represented by a set of weakly interacting subsystems where order is mostly determined by local (intraporous) constraints. The collective effects (interporous) are expected to be weak enough that the interaction among subsystems can be neglected.

The behavior of a liquid crystal phase in each independent pore segment may be explained using a simplified Landau approach. Given the 35 Å pore radius, at least 50% of the molecules are in contact with the surface. Neglecting details like biaxiality, the liquid crystal orientational order in a pore can be described by an average molecular orientation along the pore and an effective scalar order parameter Q [16], obtained by averaging over a pore. In a free energy expansion,

$$f=f_0+\tfrac{1}{2}a(T-T^*)Q^2-\tfrac{1}{3}bQ^3+\tfrac{1}{4}cQ^4+hQ^2-gQ\,, \tag{2}$$

with f_0, a, T^*, b, and c known parameters in a Landau expansion [3,16]; hQ^2 and $-gQ$ are added to describe the confinement-induced constraints (see below), similarly to what was done in less restrictive geometries to describe surface effects [3,20]. Minimization of the above free energy yields the temperature dependence of Q.

The hQ^2 term describes the disordering effects of surface-induced deformations. As these depend strongly on pore shape and the roughness of its surface, h is expected to vary from pore to pore. Introducing R as the effective radius of curvature of the surface, we estimate $h \sim L/R^2$, where L represents the Landau–de Gennes expansion coefficient characterizing all terms having derivatives of the order parameter in second order [3,4]. The $-gQ$ term describes the ordering effect of the surface interactions; g is expected to be shape independent, thus, constant throughout the system. The magnitude of g is estimated via $g=W/RS_{\rm nem}$ where W is the surface anchoring strength of the liquid crystal on the glass surface and $S_{\rm nem}$ is the bulk nematic order parameter.

The first four terms in Eq. (2) describe the bulk first order phase transition at $T_{\rm NI}=T^*+2b^2/9ac$; including hQ^2 depresses the transition temperature by $\Delta T = 2h/a = 2L/aR^2$. The effect of h may be viewed as a renormalization of T^*. Using typical values for L and a [3,4] and the average pore radius as an estimate for R, the transition temperature is shifted by ~ 30 K. The effect of $-gQ$ is similar to that of the external magnetic field on a spin system and replaces a discrete phase transition by a continuous evolution of order, becoming more gradual with increasing coupling g. Under less severe constraints (pores larger than the nematic correlation length), where the surface effect is limited to the boundary layer and is not describable by our simplified model, the NI transition is only somewhat suppressed [3–5,8,9].

Because of the pore's relatively elongated shape, the local ordering directions through a pore do not deviate considerably from the average one. For a single pore characterized by our scalar order parameter Q, Eq. (1) then yields $\Delta\nu = \Delta\nu_0 Q(3\cos^2\theta - 1)/2$, with θ the angle between the NMR field and the average ordering direction in the pore. In addition, the contribution from the orientational order to the specific heat Δc is [21] $\Delta c = aTQ|\partial Q/\partial T|$. The resulting specific heat peak near $T_{\rm NI}-2h/a$, broadened by the presence of the g term, has a width on the order g/a.

Given our approximation, the system can be represented by a Gaussian distribution $w(h)$ characterized by an average disordering parameter h_0 and width σ. This enables us to calculate the expected response functions of the total system by averaging them over $w(h)$ (process denoted by $\langle\rangle$). Further, we also neglect possible correlations between the order parameter Q and the angle θ which is taken to be randomly distributed. Each h produces an individual powder pattern [18] with FWHM given by $\Delta\nu_0 Q/2$. So, the ^{2}H-NMR spectrum is the superposition of such patterns arising from a distribution of h. The full width at half maximum $\langle\Delta\nu\rangle$ of the resulting single peak spectrum is approximately given by $\Delta\nu_0\langle Q\rangle/2$. A more detailed calculation where interconnection of the pore segments is used to describe details like the sharpness of the ^{2}H-NMR peak will be published elsewhere. Using bulk 5CB parameters (a, T^*, b, c, L) [7] and the anchoring strength $W=10^{-4}$ J/m^2 for a glass interface, the best fit of the predicted temperature dependence of the linewidth to the experimental one (Fig. 1) is obtained with $2h_0/a = 33$ K and $2\sigma/a = 17$ K. Expressing them in terms of an effective surface radius of curvature, $(L/h_0)^{1/2} \sim 28$ Å and $(L/\sigma)^{1/2} \sim 39$ Å, they are consistent with the average pore radius. The predicted behavior of the average order parameter $\langle Q\rangle$ together with Q calculated for $h=h_0$, over a broader temperature range, are shown in the inset to Fig. 1.

The orientational contribution to the heat capacity of a liquid crystal in a porous network of volume V is equally obtained by averaging as $\langle\Delta C\rangle = aVT\langle Q|\partial Q/\partial T|\rangle$, which yields a broad bump centered at about $2h_0/a$ (inset to Fig. 2). Unfortunately, our studies of 5CB in Vycor were limited to the vicinity of room temperature, where the deviation of the temperature dependence of the heat capacity C from the linearly temperature dependent background is only becoming apparent. For 5CB (inset to

Fig. 2) the orientational contribution is shown after subtraction of the high temperature background. The rise in heat capacity with cooling is in surprisingly good agreement with our prediction for $\langle \Delta C \rangle$ using h_0 and σ as determined by ^{2}H-NMR, without any additional fitting parameter. Under the same constraints, the 7CB sample, of higher T_{NI}, clearly shows the model-predicted bump (inset to Fig. 2). For 7CB, we estimate [22] the integral of ΔC per unit mass to yield 0.8 J/g. This compares well with the area under a 7CB bulk peak of 1.55 J/g [8], and the latent heat for the bulk NI transition of 2.08 J/g [23]. In 5CB, given the limited temperature range, the area under the data is 0.13 J/g, but larger if the data extended to lower temperatures. Comparing to 1.12 J/g for the area under the bulk peak and 1.56 J/g for the NI bulk latent heat [23], we are still far from the bump maximum.

The suppressed and broad bump in Vycor, in contrast to the pronounced and marginally shifted peak found at the NI transition in the 175 Å pores of Aerogel [9], can be explained in terms of its smaller pore size and narrower pore size distribution. Increasing the pore size by a factor of 3 changes h_0 by an order of magnitude, which may roughly describe the lesser temperature shift and peak suppression in Aerogel. Notice that the applicability of our model, based on an effective order parameter, is for Aerogel pore sizes more qualitative than for Vycor.

In summary, ^{2}H-NMR and calorimetric studies on nematic liquid crystals confined to Vycor glass show that the NI transition is substituted by a gradual increase of the local orientational order with decreasing temperature. This is attributed to severe constraints on the liquid crystal due to the porous network. A simplified model of independent subsystems (liquid crystals in pore segments), where the orientational order is described by an effective scalar order parameter, is used. Inclusion of ordering and disordering terms in the Landau free energy yields a satisfactory and quantitative description of the data. Comparison of the structures of Vycor and Aerogel shows that in Aerogel the interporous interaction should be stronger. A model where subsystems are affected by intraporous and interporous interactions must be used.

To establish which collective effects should be expected in random systems, it is useful to stress the distinctions and similarities with magnetic systems. Excluding polar effects, liquid crystal molecules do not distinguish between "up" and "down." Thus, the intraporous (surface-induced) orientational ordering mechanism resembles more the "random uniaxial anisotropies" than the "random fields" in the Heisenberg spin models [11]. The randomness of preferred molecular orientations in different parts of the porous network is glassylike, but, unlike spin systems [11-13], the "up-down" symmetry prevents the system from undergoing a glass to disordered state transition. Order is expected to continuously decrease with increasing temperature as in a spin system with random fields [11]. Since elastic constants are proportional to Q^2, the slowing down of long wavelength fluctuations in such systems should be caused by the decreasing interporous coupling with temperature rather than by the critical slowing down associated with the orientational glass-isotropic transition.

Detailed studies of different porous networks, liquid crystals, and surface couplings are planned together with developing a model including the interactions among molecules in different segments of the network.

We thank M. Chan for the Vycor glass and M. Gingras for useful discussions. The research was supported by NSF-STC ALCOM Grant No. DMR 89-20147 and NSF Solid State Chemistry Grant No. 91-20130. Deuterated materials were provided by S. Keast and M. Neubert through the Resource Facility of ALCOM.

---

*Permanent address: Department of Physics, University of Ljubljana, Jadranska 19, 61000 Ljubljana, Slovenia.

[1] D. Finotello *et al.*, Phys. Rev. Lett. **61**, 1954 (1988); M. H. W. Chan *et al.*, *ibid.* **61**, 1950 (1988); N. Mulders *et al.*, *ibid.* **67**, 695 (1991).

[2] B. J. Frisken, F. Ferri, and D. S. Cannell, Phys. Rev. Lett. **66**, 2754 (1991); P. Wiltzius, S. B. Dierker, and B. S. Dennis, *ibid.* **62**, 804 (1989).

[3] P. Sheng, Phys. Rev. A **26**, 1610 (1982); Phys. Rev. Lett. **37**, 1059 (1976).

[4] S. Kralj, S. Žumer, and D. W. Allender, Phys. Rev. A **43**, 2943 (1991).

[5] A. Golemme *et al.*, Phys. Rev. Lett. **61**, 2937 (1988).

[6] D. W. Allender, G. P. Crawford, and J. W. Doane, Phys. Rev. Lett. **67**, 1442 (1991); R. J. Ondris-Crawford *et al.*, Phys. Rev. Lett. **70**, 194 (1993).

[7] G. P. Crawford *et al.*, Phys. Rev. Lett. **66**, 72 (1991).

[8] G. S. Iannacchione and D. Finotello, Phys. Rev. Lett. **69**, 2094 (1992).

[9] T. Bellini *et al.*, Phys. Rev. Lett. **69**, 788 (1992).

[10] X.-l. Wu *et al.*, Phys. Rev. Lett. **69**, 470 (1992).

[11] Y. Y. Goldsmidt and A. Aharony, Phys. Rev. B **32**, 264 (1985).

[12] M. J. P. Gingras (private communication).

[13] K. Binder and A. P. Young, Rev. Mod. Phys. **58**, 801 (1986), and references therein.

[14] M. R. Kuzma *et al.*, Phys. Rev. Lett. **68**, 3436 (1992).

[15] P. Levitz *et al.*, J. Chem. Phys. **95**, 8 (1991).

[16] P. G. de Gennes, *The Physics of Liquid Crystals* (Clarendon, Oxford, 1974).

[17] M. Vilfan *et al.*, J. Chem. Phys. **89**, 597 (1988).

[18] A. Abragam, *The Principles of Nuclear Magnetism* (Clarendon, Oxford, 1962).

[19] L. M. Steele, G. S. Iannacchione, and D. Finotello, Rev. Mex. de Fis. **39**, 588 (1993).

[20] A. Poniewerski and T. J. Sluckin, in *Fluid Interfacial Phenomena,* edited by C. Croxton (Wiley, New York, 1986).

[21] M. A. Anisimov, Mol. Cryst. Liq. Cryst. **162A**, 1 (1988).

[22] ac calorimetry is not suitable to extract latent heats.

[23] J. Thoen, in *Phase Transitions in Liquid Crystals,* edited by S. Martellucci and A. N. Chester (Plenum, New York, 1992).